Annals of Pharmacy Practice and Pharmacotherapy
ISSN: 3062-4436
2021, Volume 1, Page No: 65-79

Available online at: www.galaxypub.co/page/journals

Galaxy Publication

Galaxy Publication

Elucidating the Molecular Mechanisms of Jinhong Tablets for Chronic Superficial Gastritis through Chemical Profiling and Symptom-Oriented Network Pharmacology Analysis

Olivia Chen[1], Liam O'Connell[1]*, Noah Schmidt[1]

[1]Department of Pharmaceutical Sciences, School of Pharmacy, University of North Carolina at Chapel Hill, Chapel Hill, USA.

***E-mail** ✉ liam.oconnell@outlook.com

Received: 19 January 2021; **Revised:** 16 April 2021; **Accepted:** 19 April 2021

ABSTRACT

Chronic superficial gastritis (CSG) is a widespread digestive disorder with a complex and multifactorial pathogenesis. Jinhong tablet (JHT), a traditional Chinese medicine formulation, has shown efficacy in treating CSG, but the molecular mechanisms underlying its therapeutic effects remain poorly understood. In this study, we applied ultra-performance liquid chromatography coupled with quadrupole time-of-flight tandem mass spectrometry (UPLC-Q/TOF-MS) to comprehensively profile the chemical composition of JHT. In total, 96 compounds were detected, of which 31 were validated using reference standards. Integrating these findings with symptom-oriented network pharmacology analyses—including "chi," "blood," "pain," and "inflammation"—and evaluating compound-target interaction probabilities, we identified matrix metalloproteinase 2 (MMP2), dopamine D2 receptor (DRD2), and Aldo-keto reductase family 1 member B1 (AKR1B1) as central molecular targets for JHT's action against CSG. Additionally, bioactive components belonging to alkaloids, flavonoids, and organic acids—such as chlorogenic acid (10), caffeic acid (13), (−)-corydalmine (33), (−)-isocorypalmine (36), isochlorogenic acids A, B, and C (38, 41, 47), quercetin-3-O-α-l-rhamnoside (42), quercetin (63), and kaempferol (70)—were found to exhibit notable inhibitory effects, supported by literature and molecular binding analyses. Overall, this study systematically mapped the chemical constituents of JHT and uncovered its symptom-guided molecular mechanisms in the treatment of CSG.

Keywords: Jinhong tablets, Chronic superficial gastritis, Molecular docking, Symptom-guided network pharmacology, UPLC-Q/TOF-MS

How to Cite This Article: Chen O, O'Connell L, Schmidt N. Elucidating the Molecular Mechanisms of Jinhong Tablets for Chronic Superficial Gastritis through Chemical Profiling and Symptom-Oriented Network Pharmacology Analysis. Ann Pharm Pract Pharmacother. 2021;1:65-79. https://doi.org/10.51847/TujPcvi1bS

Introduction

Chronic superficial gastritis (CSG) is a frequently encountered disorder of the gastrointestinal tract [1, 2], representing an early stage in the progression of gastric diseases. Pathologically, it is characterized by redness, swelling, and infiltration of inflammatory cells within the gastric mucosa [3], and it is commonly linked to Helicobacter pylori infection [4, 5]. Without timely intervention, CSG can evolve into serious complications, including peptic ulcers or gastric carcinoma [6]. Traditional Chinese medicine (TCM) offers distinct advantages for managing CSG, such as early therapeutic intervention, dual roles in promoting resistance and protection, and long-term recovery by modulating both microbial balance and overall physiological functions [7].

Jinhong tablet (JHT) is a classical TCM formulation derived from the historical prescription "Jinlingzi San" from the Yuan Dynasty (1271–1368 AD). It consists of four medicinal herbs: Melia toosendan (MT, Chuanlianzi), Corydalis yanhusuo (CY, Yanhusuo), Vladimiria souliei (VS, Chuanmuxiang), and Illicium dunnianum (ID, Honghuabajiao). According to TCM principles, JHT helps to harmonize liver function, relieve stagnation, regulate "chi" (qi), promote blood circulation, and alleviate gastric discomfort [8]. Clinical investigations have

demonstrated that JHT can inhibit gastric acid secretion, suppress pepsin activity, delay gastric emptying, and exhibit analgesic, antispasmodic, anti-inflammatory, and anti-ulcer effects [9]. Chemically, the main constituents of the four herbs include meliacane-type triterpenoids in MT, alkaloids in CY, sesquiterpenoids in VS, and flavonoids in ID, all of which have been shown to exert pharmacological effects against CSG [10-13] However, the therapeutic activity of JHT arises from the synergistic action of multiple compounds rather than from any single component or herb. Therefore, a detailed characterization of its chemical profile is crucial to uncover potential active compounds and their mechanisms of action.

Ultra-performance liquid chromatography coupled with electrospray ionization quadrupole time-of-flight mass spectrometry (UPLC–ESI-Q/TOF-MS) has emerged as a rapid and high-resolution approach for identifying chemical constituents in complex TCM formulations. This technique provides precise mass measurements and detailed MS/MS fragmentation data with higher efficiency compared to conventional methods, making it an ideal tool for profiling multi-component herbal medicines [14-16]

Network pharmacology offers a systems-level strategy to investigate how multi-component TCM prescriptions exert their effects [17, 18]. By integrating target prediction, bioinformatics analysis, and molecular docking, this approach enables the mapping of complex interactions among compounds, molecular targets, and signaling pathways. In CSG, JHT is believed to act on “chi” and “blood” in TCM theory and modulate “pain” and “inflammation” from a modern biomedical perspective [19, 20]. Considering the intrinsic link between symptoms and molecular targets in TCM prescriptions [21, 22], analyzing compound-target interactions through symptom-guided networks can provide deeper insights into the molecular mechanisms underlying JHT’s therapeutic efficacy.

In this study, UPLC-Q/TOF-MS was employed to systematically identify the chemical composition of JHT. Symptom-oriented network pharmacology was subsequently applied to highlight key molecular targets. Additionally, inhibitory activities from the literature, together with binding mode analyses, were used to validate compound-target interactions. This integrative approach provides a comprehensive view of JHT’s chemical profile and its molecular mechanisms in relation to CSG-associated symptoms.

Chemicals and reagents

Jinhong tablet (Batch No. 190401; Lianyungang, Jiangsu, China) and its individual herbs—MT, CY, VS, and ID—were supplied by Kanion Pharmaceutical Co., Ltd. (Lianyungang, Jiangsu, China). Reference compounds, including syringin, 4-caffeoyl quinic acid, (−)-stepholidine, (−)-scoulerin, rutin, (−)-corydalmine, (−)-isocorypalmine, cynarin, isochlorogenic acids A and C, yanhunine, (−)-tetrahydroepiberberine, (+)-isocorybulbine, (−)-tetrahydrocoptisine, (−)-tetrahydropalmatine, canadine, (+)-canadaline, 13-methyldehydrocorydalmine, dehydrocorybulbine, and 8-oxoprotoberberine were isolated and characterized in-house. Additional standards, including chlorogenic acid, vitexin-2″-O-rhamnoside, isochlorogenic acid B, protopine, (+)-corydaline, palmatine, dehydrocorydaline, costunolide, dehydrocostus lactone, toosendanin, and isotoosendanin, were procured from Chengdu Must Bio-technology Co., Ltd. (Chengdu, China). All 31 reference compounds exhibited purities exceeding 98%. LC-MS-grade solvents, including acetonitrile, methanol, and water, were obtained from Fisher Scientific (Fair Lawn, NJ, USA), and LC-MS-grade formic acid was purchased from Sigma-Aldrich (St. Louis, MO, USA). All other chemicals were of analytical grade.

Sample and standard solution preparation

To prepare the test samples, 30 mg of Jinhong tablet (JHT) powder and its four individual herbal components were accurately weighed and dissolved in 1 mL of 50% methanol. The mixture was vortexed briefly for 30 seconds and then centrifuged at 14,000 rpm for 10 minutes. The clear supernatant was collected for UPLC-Q/TOF-MS analysis. All reference compounds were separately dissolved in methanol to generate standard solutions for calibration and identification.

UPLC-Q/TOF-MS instrumentation and conditions

Chromatographic analysis was performed using an Acquity UPLC I-Class system equipped with an autosampler and binary solvent delivery. Separation was carried out on a BEH C18 column (2.1 × 100 mm, 1.7 μm) maintained at 40 °C. The mobile phase consisted of 0.1% formic acid in water (A) and 0.1% formic acid in acetonitrile (B) at a flow rate of 0.4 mL/min. Gradient elution was applied as follows: 5–30% B over 0–10 min, 30–60% B over 10–

15 min, 60–100% B over 15–19 min, hold at 100% B for 19–21 min, and return to 5% B for re-equilibration. Samples were kept at 10 °C, and two μL of solution was injected in each run.

Mass spectrometry was performed on a SYNAPT G2 HDMS Q-TOF (Waters, UK) with electrospray ionization. Operating parameters included capillary voltage of 3 kV (positive) or −2.5 kV (negative), sample cone voltage of 30 V (positive) or 40 V (negative), extraction cone 4 V, source temperature 100 °C, desolvation temperature 300 °C, cone gas 50 L/h, and desolvation gas 800 L/h. Argon was used as the collision gas in both MSE and MS^2 modes. Mass range acquisition was 50–1500 Da for positive and negative modes. Leucine enkephalin served as a lock mass reference (5 μL/min) at m/z 556.2770 (positive) or 554.2617 (negative). Data were collected in centroid mode.

Data processing

Raw data were processed using MassLynx V4.1 (Waters). Elemental compositions were predicted with a maximum mass error of 5 ppm, minimum relative intensity of 5%, and DBE between 5 and 15. Atom count limits were set as follows: C 0–60, H 0–100, O 0–50, N 0–5, and S 0–2 [23].

Identification strategy for JHT compounds

A chemical database was established based on literature, recording each compound's name, molecular formula, exact mass, and structure. From this, 667 candidate compounds were selected. Retention times and fragmentation patterns from reference standards were compiled to guide identification. Extracted ion chromatograms (EICs) were used to screen all compounds against the JHT sample. To determine the herbal origin of each detected peak, the chromatograms of the four individual herbs were compared. Peaks corresponding to known compounds were confirmed by combining fragmentation data, reference standards, and databases such as ChemSpider (http://www.chemspider.com/) and MassBank (http://www.massbank.jp/). Unidentified peaks were further analyzed to infer carbon skeletons and potential herbal sources. Diagnostic ions and MS/MS patterns were cross-checked against literature and standard references to verify the structures [24, 25].

Prediction of compound targets in JHT and CSG-associated symptoms

Three-dimensional structures of the 96 chemical constituents in Jinhong tablet (JHT) were constructed using the Schrödinger Software Suite (Schrödinger, LLC, New York, NY, 2015) and converted into SMILES format. These SMILES representations were uploaded to the SwissTargetPrediction webserver (http://www.swisstargetprediction.ch/) to predict potential human protein targets [26]. A database of predicted targets interacting with JHT compounds (database 1) was compiled. To link these targets to the symptoms of chronic superficial gastritis (CSG), the DrugBank database (https://www.drugbank.ca/) was used to identify protein targets associated with the keywords "mitochondria," "blood," "pain," and "inflammation" [27], generating a symptom-related target database (database 2). To ensure uniqueness, each protein was indexed by its UniProt ID for all subsequent analyses. Key targets were defined as proteins that were both predicted to interact with JHT constituents and implicated in CSG symptoms. In total, 301 overlapping targets from databases 1 and 2 were selected for further study.

Bioinformatics enrichment and protein-protein interaction analysis

The 301 identified targets were subjected to gene ontology (GO) and Kyoto Encyclopedia of Genes and Genomes (KEGG) enrichment analyses using Gene Set Enrichment Analysis (GSEA, version 3.0, http://software.broadinstitute.org/gsea/). Five separate target sets were analyzed: all targets, and targets associated with each of the four symptom categories ("chi," "blood," "pain," and "inflammation"). Analyses covered cellular component, molecular function, biological process, and signaling pathways, with results filtered for false discovery rate (FDR) < 0.05. For the complete target set, the top 10 enriched terms were examined for each GO category and pathway, and these were compared to the corresponding top terms in the four symptom-specific datasets. For the symptom-specific target sets, the top five GO terms for cellular component, molecular function, and biological process, and the top 10 signaling pathways, were considered.

Protein-protein interaction (PPI) networks for all five target sets were predicted using the STRING database (https://string-db.org/) with "Homo sapiens" as the species and a medium confidence threshold of > 0.4. PPI networks were visualized in Cytoscape 3.5, and key subnetworks were identified using the Molecular Complex Detection (MCODE) plugin. MCODE parameters were set as follows: degree cutoff = 2, node score cutoff = 0.2,

K-core = 2, and max depth = 100. For the full target set, significant subnetworks with MCODE scores ≥ 5 were extracted, while for the four symptom-specific sets, the most significant subnetworks with the highest MCODE scores were selected.

Screening of key targets and pharmacological network construction

Based on the SwissTargetPrediction outcomes, the likelihood of interaction between each chemical constituent and its corresponding protein targets was quantified using probability values. To assess the relative significance of each target, a cumulative score was calculated by summing the interaction probabilities across all 96 compounds:

$$Score = \sum_{k=1}^{n} Probability \quad (1)$$

(n=degree, representing the number of interacting compounds).

Targets identified in the pharmacological networks for each symptom were ordered based on their cumulative interaction scores. Those with the highest ranks were then selected as key targets. Symptom-guided networks representing “chi,” “blood,” “pain,” and “inflammation” were created in Cytoscape 3.5, illustrating the interactions between JHT constituents and their respective targets.

Molecular docking of representative compounds with key protein targets

To explore potential binding interactions, a semi-flexible docking approach—allowing ligand flexibility while keeping protein structures rigid—was carried out in Glide 6.6 (Schrödinger Software Suite, 2015). Crystal structures for Aldo-keto reductase family one member B1 (AKR1B1, UniProt ID: P15121), dopamine D2 receptor (DRD2, UniProt ID: P14416), and matrix metalloproteinase 2 (MMP2, UniProt ID: P08253) were retrieved from the Protein Data Bank (PDB IDs: 1US0, 6LUQ, 1HOV). Protein preparation included the addition of hydrogen atoms, the reconstruction of missing side chains, and energy minimization using the Protein Preparation Wizard. Binding pockets were defined by the mass centroids of their native ligands (IDD594, risperidone, SC-74020), corresponding to the catalytic or substrate-binding sites of AKR1B1, DRD2, and MMP2, respectively.

The 3D structures of ten representative compounds (10, 13, 33, 36, 38, 41, 42, 47, 63, 70) were generated and optimized using the MMFF force field at pH 7.0 ± 2.0 in the LigPrep module. Docking was performed using the standard precision (SP) protocol with 10 runs per compound-target pair. Native ligands were docked first to validate the docking method, and their scores were used as references to evaluate the binding potential of the selected compounds. The best docking score from each run was recorded for analysis, while all other settings were left at default values.

Identification and profiling of compounds in JHT via UPLC-Q/TOF-MS

Analysis of JHT by UPLC-Q/TOF-MS led to the detection of 96 chemical compounds, which included 28 alkaloids, 20 organic acids, 16 sesquiterpenoids, 13 triterpenoids, eight flavonoids, four phenylpropanoids, and seven additional components. Out of these, 31 compounds were unambiguously confirmed by comparison with authentic reference standards. The source of each identified compound was determined by matching the chromatographic profiles of the individual herbal ingredients with the overall JHT chromatogram. Base peak intensity (BPI) chromatograms were acquired in both positive and negative ion modes **(Figure 1)**.

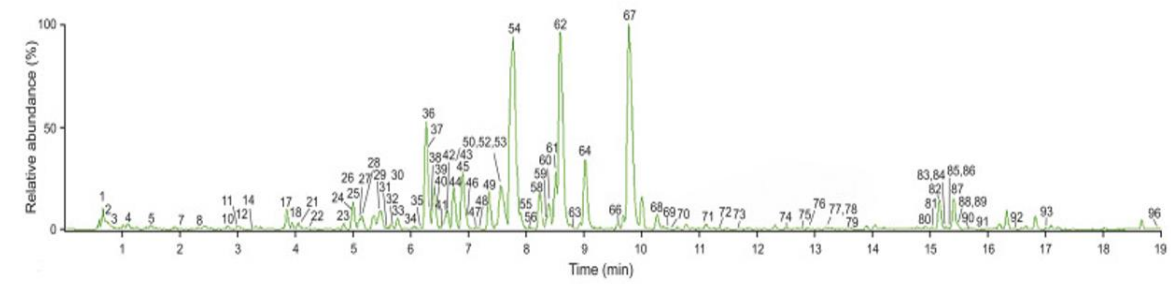

a)

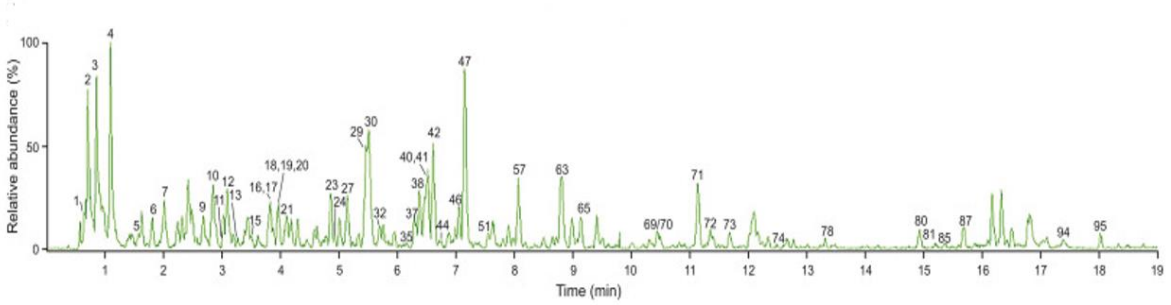

b)

Figure 1. Base Peak Intensity (BPI) Chromatograms of Jinhong Tablet (JHT). (a) Positive ion mode (+) ESI-MS chromatogram; (b) Negative ion mode (−) ESI-MS chromatogram.

Alkaloids

A total of 28 alkaloids were detected from Corydalis yanhusuo (CY) in JHT, comprising 14 tetrahydroprotoberberine alkaloids (22, 28, 31, 33, 36, 39, 43, 44, 48, 49, 53, 54, 58, 62), six protoberberine alkaloids (50, 60, 61, 64, 67, 68), two protopine alkaloids (45, 52), two aporphinoid alkaloids (34, 66), and four additional alkaloids of other types (25, 55, 59, 77), all observed in positive ion mode. Among these, 18 alkaloids—11 tetrahydroprotoberberine (22, 28, 33, 36, 43, 48, 49, 53, 54, 58, 62), four protoberberine (60, 61, 64, 67), one protopine (45), and two other alkaloids (59, 77)—were definitively confirmed using reference standards.

Flavonoids

Eight flavonoid compounds were identified in JHT, including two flavones (63, 70) and six flavonoid glycosides (23, 29, 30, 32, 37, 42). Of these, five compounds (23, 29, 32, 37, 42) were O-glucosyl flavonoids, while compound 30 was characterized as a C-glucosyl flavonoid.

Organic acids

Organic acids, defined by the presence of a carboxyl functional group, formed another major component class in JHT. Twenty organic acids were detected, including eight caffeoylquinic acids (8, 9, 11, 21, 38, 40, 41, 47), three coumaroylquinic acids (10, 17, 20), two phenolic acids (7, 14), and seven other acid derivatives (2, 3, 4, 27, 35, 46, 57).

Triterpenoids

Thirteen triterpenoids (69, 73, 80, 81, 84, 85, 86, 88, 90, 91, 94, 95, 96) were identified, all of limonoid type and uniquely derived from Melia toosendan (MT).

Sesquiterpenoids

Sixteen sesquiterpenoids were detected in JHT. Compounds 71, 72, 74, 75, 78, 79, 82, 83, 87, 89, 92, and 93 originated from Vladimiria souliei (VS), while compounds 8, 14, 26, and 65 were derived from Illicium dunnianum (ID).

Compound 62 is presented as an example of the identification process. This compound eluted at 8.58 min, exhibiting an [M+H]+ ion at m/z 370.2030 corresponding to the molecular formula C22H28NO4. Fragment ions at m/z 192.1030 (C11H14NO2) and 179.1068 (C11H15O2) were generated via retro-Diels–Alder (RDA)

cleavage, while the ion at m/z 165.0924 resulted from B-ring cleavage. Sequential losses of CH4 (16.0313 Da) and CO (27.9949 Da) produced ions at m/z 354.1710 and 326.1754, indicating adjacent methoxy substitutions [28]. Additional high-energy MSE fragment ions at m/z 176.0719, 149.0605, 148.0771, 135.0811, and 121.0664 were also observed. Because compound 62 matched the retention time and fragmentation pattern of the authentic (+)-corydaline standard, it was conclusively identified as (+)-corydaline. Other tetrahydroprotoberberine alkaloids were characterized by comparing their fragmentation pathways to that of compound 62.

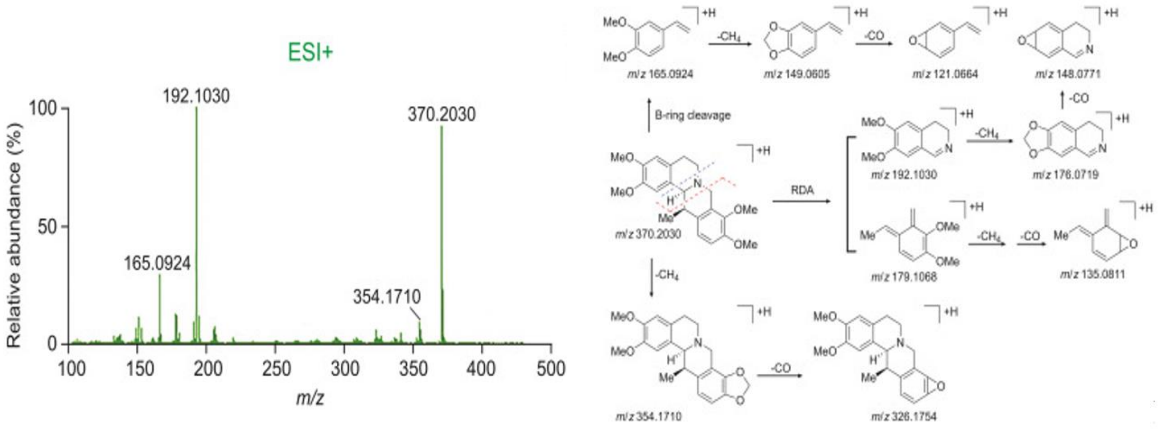

a) b)

Figure 2. Detailed fragmentations and proposed fragment pathway for compound 62.

Construction of a symptom-oriented target database and bioinformatics analysis of JHT-associated targets

During the clinical application of JHT for treating chronic stomach gastritis (CSG), the stomach—the primary target organ—can directly interact with the herbal components of JHT. To explore this, we compiled all identified compounds to establish a pharmacological network for JHT and examined its therapeutic mechanisms against CSG through four symptom categories: "chi," "blood," "pain," and "inflammation." The concept of "Chi," also defined as "vital energy," was primarily linked to mitochondrial functions related to energy production, and was therefore designated as "mitochondria" during target collection [29, 30]. As illustrated in **Figure 3a**, the target collection process combined predictions from the SwissTargetPrediction server with symptom-based target searches in the DrugBank database. SwissTargetPrediction analysis identified 1,136 protein targets, forming multiple interactions with 96 compounds. Meanwhile, DrugBank searches yielded 249 targets associated with "chi," 96 with "blood," 408 with "pain," and 140 with "inflammation." Overlapping targets from the two approaches were extracted for each symptom as presented in **Figure 3b**. In total, 35 targets for "chi," 40 for "blood," 192 for "pain," and 74 for "inflammation" were found to interact with JHT compounds, suggesting these proteins may underlie the pharmacological effects of JHT in CSG treatment.

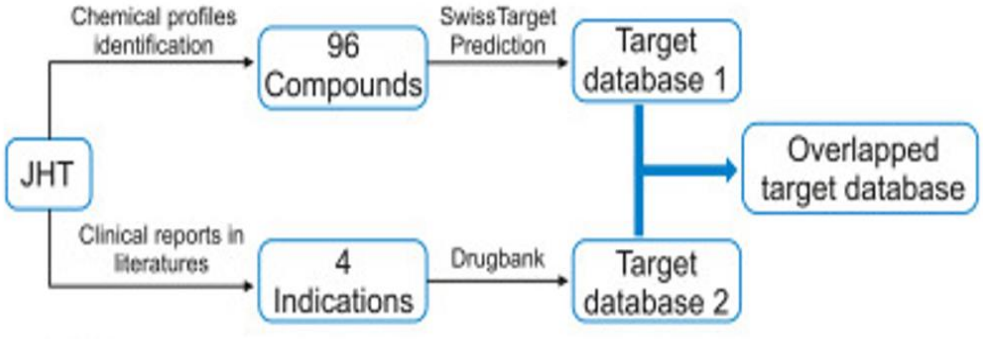

a)

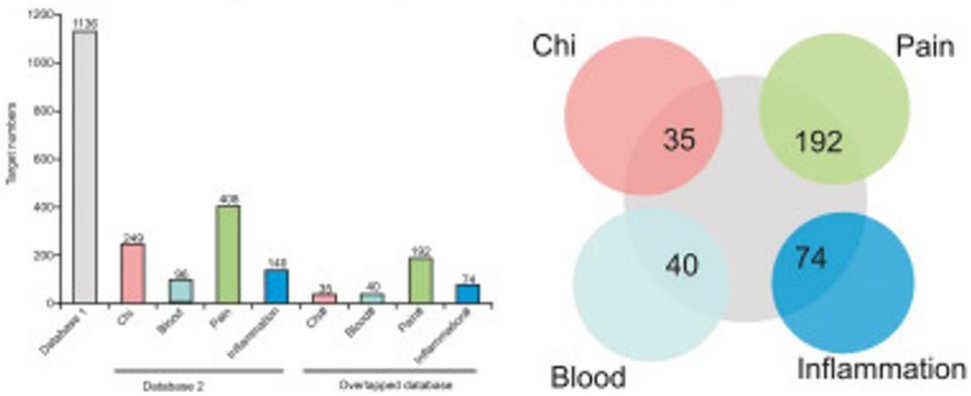

b)

Figure 3. Symptom-oriented target database for the therapeutic effects of JHT in chronic superficial gastritis (CSG). (a) Workflow for target collection integrating predictions from the SwissTargetPrediction server with symptom-based searches in the DrugBank database. (b) Number of targets in database 1, database 2, and their overlap. The overlapped regions for "Chi#," "Blood#," "Pain#," and "Inflammation#" represent the shared targets between the two databases for each symptom.

To explore the biological mechanisms underlying JHT's therapeutic effects against CSG, non-redundant target datasets corresponding to the four CSG-related symptoms were subjected to gene set enrichment analysis (GSEA). The associations between enriched biological items and symptoms were subsequently evaluated. As shown in **Figure 4**, the top 10 terms for molecular function, cellular component, biological process, and signaling pathways were selected based on P-value ranking. Among biological processes, responses to compounds—such as oxygen-containing molecules, organic cyclic compounds, nitrogen-containing molecules, and endogenous stimuli—were predominant **(Figure 4a)**. The most prominent process, "response to oxygen-containing compound," suggests that the metabolism or regulation of these molecules may influence "chi" and "pain."

Analysis of cellular components and molecular functions indicated that targets were mainly localized to membrane regions and neural structures, including synapses, neurons, and dendritic trees, which modulate the activity of molecular transducers, receptors, kinases, and gated channels **(Figures 4b and 4c)**. The most significant terms were "intrinsic component of plasma membrane" for cellular components and "molecular transducer activity" for molecular function. KEGG pathway analysis identified "neuroactive ligand-receptor interaction" as the key signaling pathway, aligning with the cellular component and molecular function results **(Figure 4d)**.

When analyzed by symptom, the most relevant pathways were "pathways in cancer" for "chi," "complement and coagulation cascades" for "blood," "neuroactive ligand-receptor interaction" for "pain," and "protein serine/threonine kinase activity" for "inflammation", showing strong symptom-specific correlations. Overall, the gene enrichment results indicate that individual pathways may relate to multiple symptoms, and the integrated interactions among these biological items collectively support the therapeutic effects of JHT against CSG.

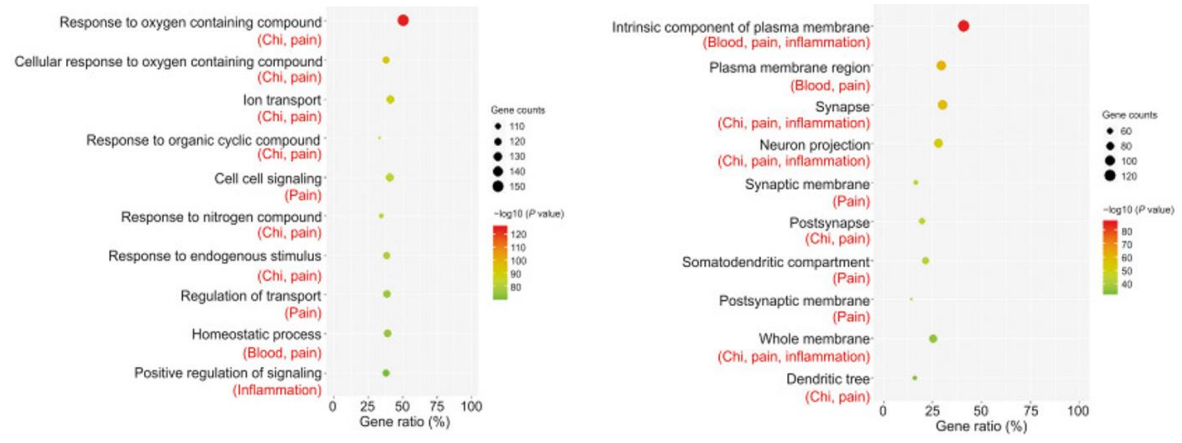

a) b)

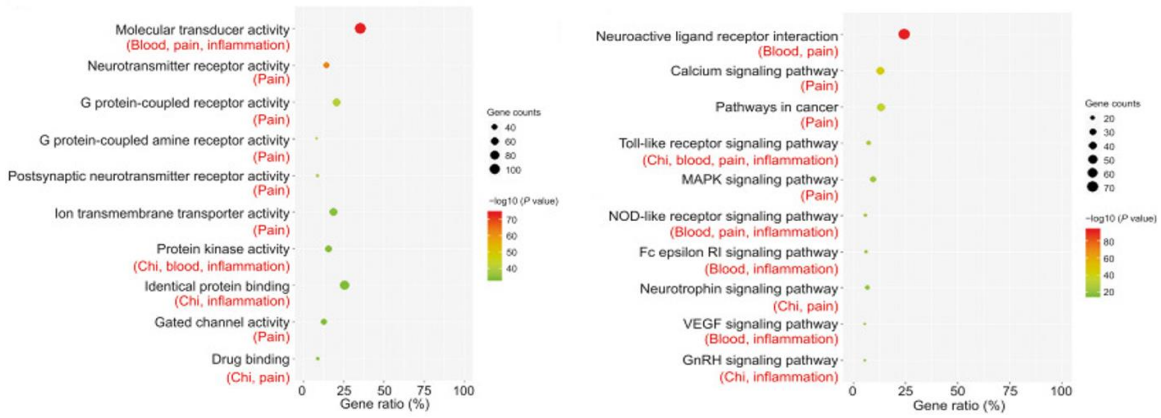

c) d)

Figure 4. Gene enrichment analysis of 301 non-redundant targets contributing to JHT's therapeutic effects against CSG. (a) Top 10 terms in GO biological process. (b) Top 10 terms in the GO cellular component. (c) Top 10 terms in the GO molecular function. (d) Top 10 terms in KEGG signaling pathways. The four associated symptoms—chi, blood, pain, and inflammation—are indicated below each item.

Protein-protein interaction analysis of the 301 non-redundant targets revealed five key subnetworks with MCODE scores ≥ 5, as **(Figure 5)**, each containing targets linked to one or more of the four symptoms. Targets associated with multiple symptoms included: subnetwork 1: PTGDR2, GPR55, GPER1, APP, CNR2; subnetwork 2: BCL2L1, NR3C1, NOS2, CASP1, LTB4R, F2, PPARG, VCAM1, MMP2, IL1B; subnetwork 3: PLG, ALOX5, IKBKB, PTGS2, ALB, VEGFA, IL6, PGR, MAPK14, SYK; subnetwork 4: GSR; subnetwork 5: ALOX15, BCL2.

Examining the most significant subnetworks for each symptom dataset, GPER1 was identified in the "chi" subnetwork; F2, MMP2, ALB, VEGFR, IL6, and MAPK14 in the "blood" subnetwork; PTGDR2, GPR55, and CNR2 in the "pain" subnetwork; and NOS2, CASP1, IL1B, PLG, SYK, PPARG, VCAM1, ALOX5, IKBKB, and PTGS2 in the "inflammation" subnetwork. These proteins represent the central hubs within the protein-protein interaction networks corresponding to the four symptom categories.

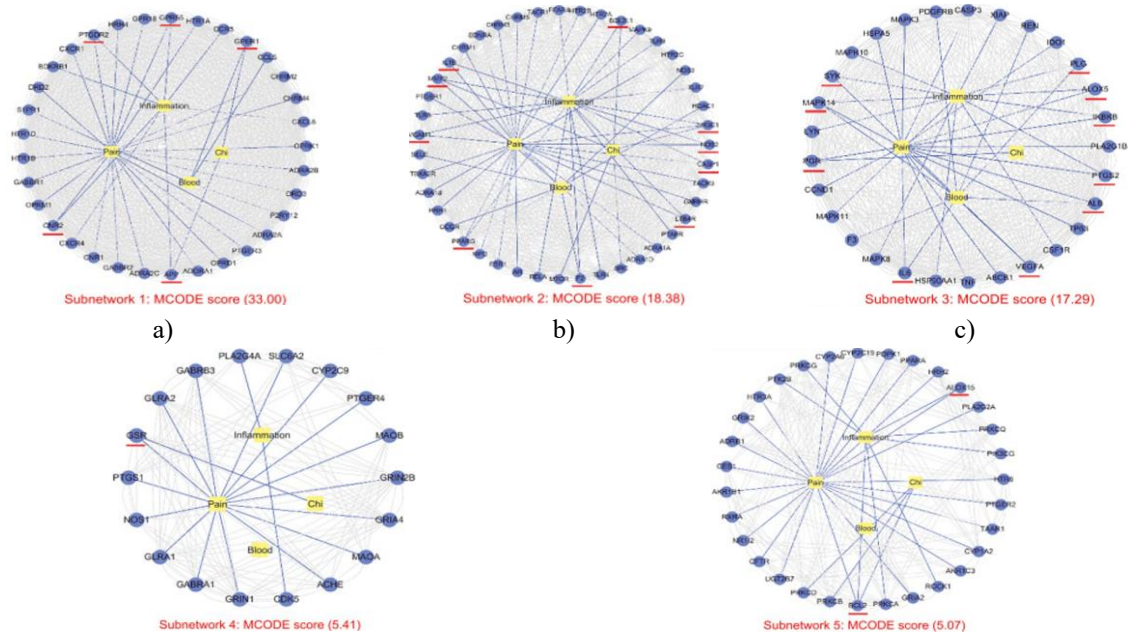

a) b) c)

d) e)

Figure 5. Key PPI subnetworks of non-redundant targets (301 targets) contributing to the therapeutic action of JHT against CSG. Five subnetworks with MCODE scores ≥ 5 were identified, and targets participating in more than one symptom are highlighted in red.

Screening of targets in the symptom-oriented pharmacological network for JHT

The symptom-specific pharmacological networks for "chi," "blood," "pain," and "inflammation" revealed that the principal targets for each symptom interacted with multiple compounds from the four constituent herbs of JHT, including alkaloids, flavonoids, organic acids, and sesquiterpenoids. Potential interactions between targets and compounds were quantified as weight factors to prioritize targets for each symptom. Those with higher scores were selected to represent the core regulatory effects of JHT.

From **Table 1** the top three targets for each symptom-based network were identified as follows: SIGMAR1, MMP2, and APP for "chi"; F3, MMP2, and SYK for "blood"; MMP2, APP, and ALOX5 for "inflammation"; and DRD1, DRD2, and AKR1B1 for "pain." MMP2 emerged as a recurring hub in "chi," "blood," and "inflammation," reflecting its multifaceted roles in vascular remodeling, angiogenesis, tissue repair, inflammation, tumor progression, and atherosclerotic plaque destabilization [31]. Prior research has also shown MMP2 expression differs significantly between gastritis and healthy gastric tissues [32-34], underscoring its potential as a biomarker.

To examine the overlap between gastritis-related targets and the effects of JHT, a "gastritis-targets-symptoms" network was generated **(Figure 6a)**, based on FDA-approved gastritis drug targets reported in OMIM and DrugBank [35]. Fourteen targets were shared between the 90 gastritis-associated proteins and the 107 symptom-related targets: CHRM1, CHRM4, TYMS, DRD3, DRD2, TUBB1, HTR1A, HTR2A, PTGS1, PTGS2, AKR1B1, MPO, XDH, and SLC18A2. All but TYMS were linked to "pain," highlighting it as the dominant symptom targeted by approved gastritis medications. Notably, DRD2 and AKR1B1 were among the top-ranking targets in the "pain" network. These findings indicate that when JHT is used to treat CSG, MMP2, DRD2, and AKR1B1 are likely central targets through which the formula alleviates multiple symptoms, including "chi," "blood," "pain," and "inflammation."

Table 1. Detailed information for the screened targets involved in chronic superficial gastritis (CSG)-associated symptoms, such as "chi," "blood," "pain," and "inflammation," based on scoring evaluation and an analysis of their association with gastritis.

Gene name	Protein class	Symptoms	Degree[a]	Score[b]	Selection standard[c]
SIGMAR1	Membrane receptor	Chi	41	12.02	Top 3 target for symptom
MMP2	Protease	Chi, blood, inflammation	34	6.70	Top 3 target for symptom
APP	Membrane receptor	Chi, inflammation	26	5.67	Top 3 target for symptom
F3	Protease	Blood	38	13.04	Top 3 target for symptom
SYK	Kinase	Blood	34	2.84	Top 3 target for symptom
ALOX5	Oxidoreductase	Inflammation	37	5.56	Top 3 target for symptom
DRD1	Family A GPCR	Pain	25	13.68	Top 3 target for symptom
DRD2	Family A GPCR	Pain	35	13.47	Top 3 target for symptom, drug target for gastritis
AKR1B1	Enzyme	Pain	41	14.41	Top 3 target for symptom, drug target for gastritis
CHRM1	Family A GPCR	Pain	24	1.87	Drug target for gastritis
CHRM4	Family A GPCR	Pain	32	4.16	Drug target for gastritis
TYMS	Transferase	Chi	36	1.54	Drug target for gastritis
DRD3	Family A GPCR	Pain	33	11.20	Drug target for gastritis
TUBB1	Structural protein	Pain	20	1.42	Drug target for gastritis
HTR1A	Family A GPCR	Pain	33	10.20	Drug target for gastritis
HTR2A	Family A GPCR	Pain	38	4.44	Drug target for gastritis
PTGS1	Oxidoreductase	Pain	37	1.73	Drug target for gastritis
PTGS2	Oxidoreductase	Pain, inflammation	54	4.07	Drug target for gastritis
MPO	Enzyme	Pain	19	1.96	Drug target for gastritis
XDH	Oxidoreductase	Pain	8	2.64	Drug target for gastritis
SLC18A2	Electrochemical transporter	Pain	18	1.60	Drug target for gastritis

a. The number of JHT compounds that are predicted to interact with a given target.

b. A score calculated by summing the probabilities of interactions between a target and its associated compounds.

c. Target selection was based on two criteria: (1) being among the top three targets according to the scoring evaluation for each symptom, and (2) having a documented association with gastritis in the DrugBank and OMIM databases.

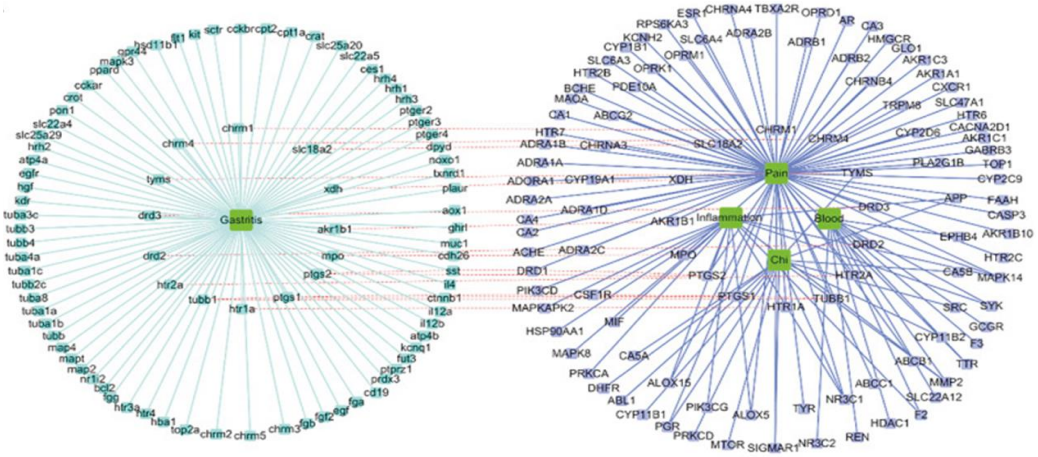

Figure 6. Key targets and signaling pathways linked to gastritis. (a) The network connecting gastritis with its associated targets and the four relevant symptoms—"chi," "blood," "pain," and "inflammation"—is illustrated. In this network, gastritis is represented by green nodes, its targets by blue nodes, and symptom-related targets by cyan nodes. Labels for gastritis appear in lowercase, whereas symptom-related targets are in uppercase; red dashed lines indicate interactions between the features. (b) Major signaling pathways influenced by MMP2, DRD2, and AKR1B1. Pathways strongly associated with gastritis are highlighted in bold red and linked by red dashed lines.

Analysis of GSEA results revealed signaling pathways involving these three targets. MMP2 was linked to four pathways, including the "leukocyte transendothelial migration" pathway, which is known to facilitate T-cell infiltration into the gastric mucosa during Helicobacter pylori infection, a key factor in active chronic gastritis [36]. Suppression of MMP2 may therefore inhibit this pathway, contributing to a protective effect on gastric tissue. DRD2 was implicated in two pathways, notably the "neuroactive ligand-receptor interaction," where dopamine-DRD2 signaling modulates nociceptive responses [37]. Clinically, DRD2 antagonists such as domperidone are effective in relieving nausea and vomiting in chronic gastroparesis and in promoting gastric emptying [38, 39]. AKR1B1 was associated solely with the "folate biosynthesis" pathway, which governs BH4 (tetrahydrobiopterin) production. Studies in mice indicate that excessive BH4 from axotomized neurons and infiltrating macrophages can heighten pain sensitivity [40]; thus, inhibition of AKR1B1 may reduce nerve injury-induced hyperalgesia without impacting normal pain perception. Together, these results suggest that MMP2, DRD2, and AKR1B1 act through distinct pathways that can be modulated by compounds in JHT to mitigate gastritis symptoms.

Inhibitory potential of representative JHT compounds against MMP2, DRD2, and AKR1B1, and structural binding analysis

Compounds predicted with full interaction probability (1.0) for MMP2, DRD2, and AKR1B1 were selected from SwissTargetPrediction. Their experimentally determined inhibitory activities were obtained from the ChEMBL database (https://www.ebi.ac.uk/chembl/) [41-45] and are summarized in **Table 2**. A refined pharmacological

network linking herbs, compounds, targets, and symptoms was then constructed to illustrate the multi-level mechanism of JHT in CSG therapy. Furthermore, the binding modes of both native ligands and representative JHT compounds with MMP2, DRD2, and AKR1B1 were examined in detail and visualized in **Figures 7b–7d**, providing structural insight into their interactions and potential inhibitory mechanisms.

Table 2. Chemical components of JHT that could interact with MMP2, DRD2, and AKR1B1 and their validated activities.

Compounds	Structural types	Targets[a]	Possibilities[b]	Inhibitory activities[c] (nM)	Refs.
Chlorogenic acid (10)	Organic acids	AKR1B1	1.00	300	[41]
Caffeic acid (13)	Organic acids	MMP2	1.00	24.26	[42]
(−)-Corydalmine (33)	Alkaloids	DRD2	1.00	N/A[d]	N/A
(−)-Isocorypalmine (36)	Alkaloids	DRD2	1.00	N/A	N/A
Isochlorogenic acid C (38)	Organic acids	AKR1B1	1.00	N/A	N/A
Isochlorogenic acid A (41)	Organic acids	AKR1B1	1.00	88	[41]
Quercetin-3-*O*-α-l-rhamnoside (42)	Flavonoids	AKR1B1	1.00	150	[43]
Isochlorogenic acid B (47)	Organic acids	AKR1B1	1.00	78	[41]
Quercetin (63)	Flavonoids	MMP2/AKR1B1	1.00	6680/2200	[44, 45]
Kaempferol (70)	Flavonoids	AKR1B1	1.00	10,000	[45]

a. A single compound can potentially engage with multiple targets.
b. The predicted likelihood of interaction between each compound and target; a score of 1.00 denotes a confirmed interaction according to SwissTargetPrediction.
c. The inhibitory potency (IC_{50}) of compounds against targets, obtained from the ChEMBL database (https://www.ebi.ac.uk/chembl/) and relevant scientific publications.
d. "N/A" indicates that IC_{50} data are not available.

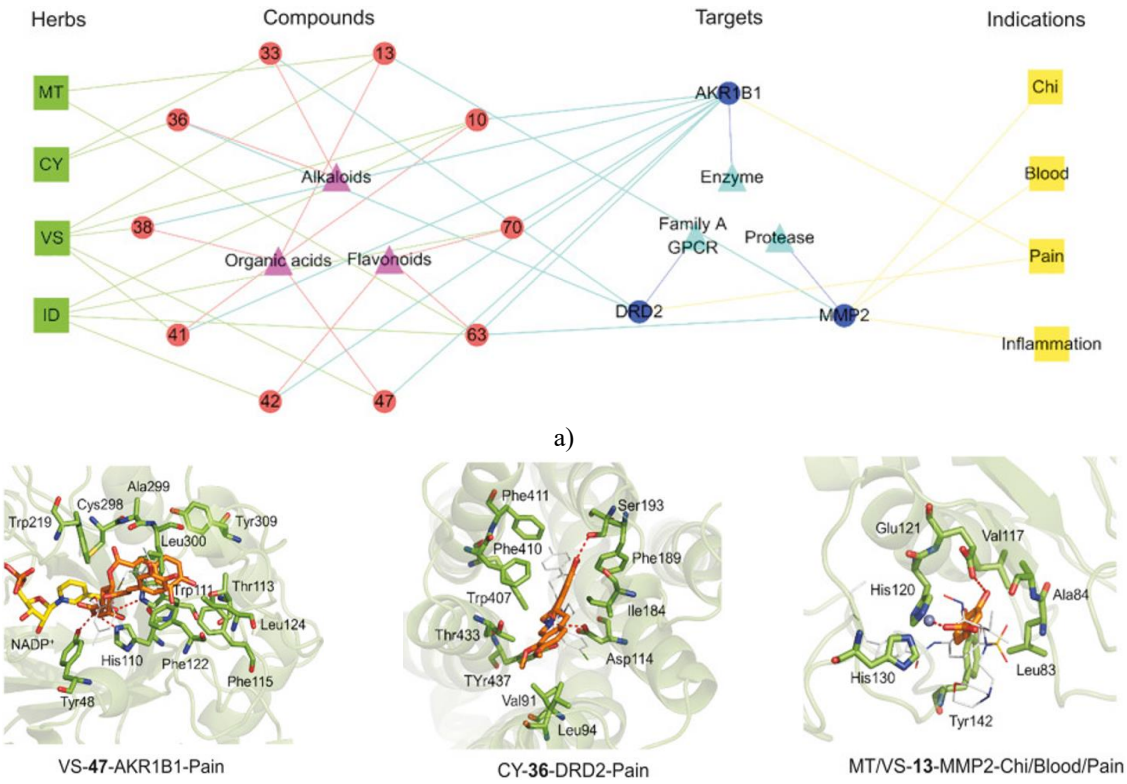

Figure 7. Refined pharmacological network of JHT and interactions between representative compounds and key targets (MMP2, DRD2, AKR1B1). (a) The network illustrates relationships among herbs, bioactive compounds, targets, symptoms, compound classes, and target types. Node shapes and colors indicate

category: herbs (green squares), compounds (red circles), targets (blue circles), symptoms (yellow squares), compound classes (purple triangles), and target types (cyan triangles), with edges color-coded to indicate the type of interaction. (b–d) Molecular binding of representative compounds with the three targets. Isochlorogenic acid B (47) bound to AKR1B1 (b), (−)-isocorypalmine (36) to DRD2 (c), and caffeic acid (13) to MMP2 (d). Native ligands, cofactors, target residues, and compounds are distinguished by colors and stick/line representations, with hydrogen bonds and electrostatic interactions highlighted as red dashed lines.

Several organic acids and flavonoids—including chlorogenic acid (10), isochlorogenic acid A (41), quercetin-3-O-α-l-rhamnoside (42), isochlorogenic acid B (47), quercetin (63), and kaempferol (70)—showed inhibitory activity against AKR1B1 with IC_{50} values ranging from 78 to 10,000 nM **(Table 2)**. These compounds predominantly occupied the catalytic pocket near the NADP+ cofactor. Isochlorogenic acid B (47) interacted with key residues such as Tyr48, His110, and Trp111, forming hydrogen bonds, while engaging additional residues (Thr113, Phe115, Phe122, Leu124, Trp219, Cys298, Ala299, Leu300, Tyr309) to stabilize binding **(Figure 7b)**.
The tetrahydroprotoberberine alkaloids (−)-corydalmine (33) and (−)-isocorypalmine (36) targeted DRD2, consistent with previous reports showing antagonistic effects of structural analogs [46]. These compounds predominantly bound within the receptor's seven-transmembrane helical substrate-binding pocket. Specifically, (−)-isocorypalmine (36) interacted with Val91, Ala94, Asp114, Ile184, Phe189, Ser193, Trp407, Phe410, Phe411, Thr433, and Tyr437, forming hydrogen bonds and electrostatic interactions at Ser193 and Asp114 **(Figure 7c)**.
Caffeic acid (13) and quercetin (63) inhibited MMP2, with IC_{50} values of 24.26 nM and 6680 nM, respectively **(Table 2)**, targeting the catalytic site adjacent to the Zn^{2+} cofactor. Caffeic acid (13) formed hydrogen bonds with Glu121 and electrostatic interactions with Zn^{2+}, while engaging residues Leu83, Ala84, Val117, His120, His130, and Tyr142 **(Figure 7d)**.
Collectively, organic acids and flavonoids were primarily responsible for the inhibition of AKR1B1 and MMP2, whereas alkaloids acted as DRD2 antagonists. These three compound classes represent the principal bioactive constituents in JHT. Pharmacological investigations of chlorogenic acid (10) [47, 48], caffeic acid (13) [49, 50], (−)-corydalmine (33), (−)-isocorypalmine (36) [51, 52], quercetin (63) [53], and kaempferol (70) [54, 55] demonstrate a clear link between the inhibitory activities of these compounds and the therapeutic outcomes of JHT in gastritis. The integrated interactions of these compounds with MMP2, DRD2, and AKR1B1 provide a mechanistic basis for the multi-target, symptom-relieving effects of JHT.

Biological insights from bioinformatics and implications for novel therapeutics in CSG
Traditional Chinese medicine (TCM) formulations typically consist of multiple herbs, making it challenging to link their therapeutic effects to specific molecular mechanisms. By leveraging data on approved drugs and their known targets from the DrugBank database (https://go.drugbank.com/), it becomes possible to correlate the symptom-specific effects of Chinese herbs with the pharmacological actions of conventional Western medications. In TCM theory, many herbal remedies exert effects related to "chi," "blood," "pain," and "inflammation." Therefore, collecting targets based on these symptom categories provides a useful framework for evaluating other TCM formulations containing herbs with similar therapeutic properties.
To elucidate the molecular mechanism of JHT in treating chronic superficial gastritis (CSG), key targets were identified. Notably, AKR1B1, DRD2, and MMP2 are closely associated with gastritis. Interaction of JHT compounds with these targets regulates biological pathways such as "leukocyte transendothelial migration," "neuroactive ligand-receptor interaction," and "folate biosynthesis," which influence pathophysiological factors of CSG, including Helicobacter pylori infection, chronic gastroparesis, and BH4-mediated neuropathic and inflammatory pain. Inhibiting these factors through JHT compounds likely produces synergistic therapeutic effects. Several constituents of JHT demonstrated inhibitory activity against AKR1B1, DRD2, and MMP2, establishing a direct pharmacodynamic link to gastritis and suggesting their potential as quality markers for evaluating JHT preparations.

Conclusion

This study systematically characterized the chemical composition of JHT using UPLC-Q-TOF/MS and explored its molecular mechanisms through a symptom-guided network pharmacology approach. Ninety-six compounds were identified in JHT, including 28 alkaloids, 20 organic acids, 16 sesquiterpenoids, 13 triterpenoids, eight

flavonoids, four phenylpropanoids, and seven other compounds, with 31 constituents confirmed against reference standards. Symptom-guided network analysis highlighted MMP2, DRD2, and AKR1B1 as critical targets mediating the therapeutic effects of JHT in CSG. Compounds such as chlorogenic acid (10), caffeic acid (13), (−)-corydalmine (33), (−)-isocorypalmine (36), isochlorogenic acid C (38), isochlorogenic acid A (41), quercetin-3-O-α-l-rhamnoside (42), isochlorogenic acid B (47), quercetin (63), and kaempferol (70) exhibited broad-spectrum activity against gastritis by interacting with these key targets and modulating the four symptom categories. Overall, this integrated approach provides a clear link between the chemical constituents of JHT and its therapeutic actions against CSG, offering a foundation for further clinical investigation and application of JHT.

Acknowledgments: None

Conflict of Interest: None

Financial Support: None

Ethics Statement: None

References

1. Fang JY, Du YQ, Liu WZ, Ren JL, Li YQ, Chen XY, et al. Chinese consensus on chronic gastritis (2017, Shanghai). J Dig Dis. 2018;19(4):182-203.
2. Sipponen P, Maaroos HI. Chronic gastritis. Scand J Gastroenterol. 2015;50(6):657-67.
3. Stolte M, Meining A. The updated Sydney system: classification and grading of gastritis as the basis of diagnosis and treatment. Can J Gastroenterol Hepatol. 2001;15(9):591-8.
4. Kuipers EJ, Uyterlinde AM, Peña AS, Roosendaal R, Pals G, Nelis GF, et al. Long-term sequelae of Helicobacter pylori gastritis. Lancet. 1995;345(8964):1525-8.
5. Varbanova M, Frauenschläger K, Malfertheiner P. Chronic gastritis - an update. Best Pract Res Clin Gastroenterol. 2014;28(6):1031-42.
6. Osaki LH, Bockerstett KA, Wong CF, Ford EL, Madison BB, DiPaolo RJ, et al. Interferon-γ directly induces gastric epithelial cell death and is required for progression to metaplasia. J Pathol. 2019;247(4):513-23.
7. Wang XL. Re-discussing the advantage of TCM in treating infectious diseases. J Tianjin Univ Tradit Chin Med. 2011;30:193-5.
8. Chen F. Clinical observation on treatment of chronic superficial gastritis with Jinhong tablets and ranitidine. Chin J Clin Ration Drug Use. 2010;3:69.
9. Zhang J, Song J, Zhang L, Ding K. Observation on therapeutic effect of 325 cases of chronic superficial gastritis with disharmony of liver and stomach treated by Jinhong tablets. Chin J Tradit Med Sci Technol. 1998;5:251.
10. Matsuda H, Tokuoka K, Wu J, Tanaka T, Kubo M. Inhibitory effects of methanolic extract from corydalis tuber against types I-IV allergic models. Biol Pharm Bull. 1995;18(7):963-7.
11. Kubo M, Matsuda H, Tokuoka K, Ma S, Shiomoto H. Anti-inflammatory activities of methanolic extract and alkaloidal components from Corydalis tuber. Biol Pharm Bull. 1994;17(2):262-5.
12. Zheng H, Chen Y, Zhang J, Wang L, Jin Z, Huang H, et al. Evaluation of protective effects of costunolide and dehydrocostuslactone on ethanol-induced gastric ulcer in mice based on multi-pathway regulation. Chem Biol Interact. 2016;250:68-77.
13. Xie F, Zhang M, Zhang CF, Wang ZT, Yu BY, Kou JP. Anti-inflammatory and analgesic activities of ethanolic extract and two limonoids from Melia toosendan fruit. J Ethnopharmacol. 2008;117(3):463-6.
14. Shi T, Yao Z, Qin Z, Ding B, Dai Y, Yao X. Identification of absorbed constituents and metabolites in rat plasma after oral administration of Shen-Song-Yang-Xin using ultra-performance liquid chromatography combined with quadrupole time-of-flight mass spectrometry. Biomed Chromatogr. 2015;29(9):1440-52.
15. Geng JL, Dai Y, Yao ZH, Qin ZF, Wang XL, Qin L, et al. Metabolites profile of Xian-Ling-Gu-Bao capsule, a traditional Chinese medicine prescription, in rats by ultra performance liquid chromatography coupled with quadrupole time-of-flight tandem mass spectrometry analysis. J Pharm Biomed Anal. 2014;96:90-103.
16. Qin ZF, Dai Y, Yao ZH, He LL, Wang QY, Geng JL, et al. Study on chemical profiles and metabolites of

Allii Macrostemonis Bulbus as well as its representative steroidal saponins in rats by ultra-performance liquid chromatography coupled with quadrupole time-of-flight tandem mass spectrometry. Food Chem. 2016;192:499-515.
17. Hopkins AL. Network pharmacology. Nat Biotechnol. 2007;25(10):1110-1.
18. Hopkins AL. Network pharmacology: the next paradigm in drug discovery. Nat Chem Biol. 2008;4(11):682-90.
19. Zhu W, Fan Z, Liu G, Yan J, Zhong T, Zheng W, et al. Symptom clustering in chronic gastritis based on spectral clustering. J Tradit Chin Med. 2014;34(4):504-10.
20. Wang Q, Yao S. Molecular basis for cold-intolerant yang-deficient constitution of traditional Chinese medicine. Am J Chin Med. 2008;36(5):827-34.
21. Li S, Zhang ZQ, Wu LJ, Zhang XG, Li YD, Wang YY. Understanding ZHENG in traditional Chinese medicine in the context of neuro-endocrine-immune network. IET Syst Biol. 2007;1(1):51-60.
22. Li S. Exploring traditional chinese medicine by a novel therapeutic concept of network target. Chin J Integr Med. 2016;22(9):647-52.
23. Wang K, Chai L, Feng X, Liu Z, Liu H, Ding L, et al. Metabolites identification of berberine in rats using ultra-high performance liquid chromatography/quadrupole time-of-flight mass spectrometry. J Pharm Biomed Anal. 2017;139:73-86.
24. Dai C, Wang C, Zhang C, Wang G, Wang J, Chen J, et al. A reference substance free diagnostic fragment ion-based approach for rapid identification of non-target components in Pudilan Xiaoyan oral liquid by high resolution mass spectrometry. J Pharm Biomed Anal. 2016;124:79-92.
25. He L, Qin Z, Li M, Chen Z, Zeng C, Yao Z, et al. Metabolic profiles of ginger, a functional food, and its representative pungent compounds in rats by ultraperformance liquid chromatography coupled with quadrupole time-of-flight tandem mass spectrometry. J Agric Food Chem. 2018;66(34):9010-33.
26. Daina A, Michielin O, Zoete V. SwissTargetPrediction: updated data and new features for efficient prediction of protein targets of small molecules. Nucleic Acids Res. 2019;47(W1):W357-W64.
27. Wishart DS, Feunang YD, Guo AC, Lo EJ, Marcu A, Grant JR, et al. DrugBank 5.0: a major update to the DrugBank database for 2018. Nucleic Acids Res. 2018;46(D1):D1074-D82.
28. Qing ZX, Cheng P, Liu XB, Liu YS, Zeng JG. Systematic identification of alkaloids in Macleaya microcarpa fruits by liquid chromatography tandem mass spectrometry combined with the isoquinoline alkaloids biosynthetic pathway. J Pharm Biomed Anal. 2015;103:26-34.
29. Wallace DC. Mitochondria as chi. Genetics. 2008;179(2):727-35.
30. Picard M, Wallace DC, Burelle Y. The rise of mitochondria in medicine. Mitochondrion. 2016;30:105-16.
31. Singh D, Srivastava SK, Chaudhuri TK, Upadhyay G. Multifaceted role of matrix metalloproteinases (MMPs). Front Mol Biosci. 2015;2:19.
32. Bergin PJ, Anders E, Sicheng W, Erik J, Jennie A, Hans L, et al. Increased production of matrix metalloproteinases in Helicobacter pylori-associated human gastritis. Helicobacter. 2004;9(3):201-10.
33. Rautelin HI, Oksanen AM, Veijola LI, Sipponen PI, Tervahartiala TI, Sorsa TA, et al. Enhanced systemic matrix metalloproteinase response in Helicobacter pylori gastritis. Ann Med. 2009;41(3):208-15.
34. Sampieri CL, de la Peña S, Ochoa-Lara M, Zenteno-Cuevas R, León-Córdoba K. Expression of matrix metalloproteinases 2 and 9 in human gastric cancer and superficial gastritis. World J Gastroenterol. 2010;16(12):1500-5.
35. Yu G, Wang W, Wang X, Xu M, Zhang L, Ding L, et al. Network pharmacology-based strategy to investigate pharmacological mechanisms of Zuojinwan for treatment of gastritis. BMC Complement Altern Med. 2018;18(1):292.
36. Enarsson K, Brisslert M, Backert S, Quiding-Järbrink M. Helicobacter pylori induces transendothelial migration of activated memory T cells. Infect Immun. 2005;73(2):761-9.
37. Potvin S, Grignon S, Marchand S. Human evidence of a supra-spinal modulating role of dopamine on pain perception. Synapse. 2009;63(5):390-402.
38. Sturm A, Holtmann G, Goebell H, Gerken G. Prokinetics in patients with gastroparesis: a systematic analysis. Digestion. 1999;60(5):422-7.
39. Abrahamsson H. Treatment options for patients with severe gastroparesis. Gut. 2007;56(6):877-83.
40. Latremoliere A, Latini A, Andrews N, Cronin SJ, Fujita M, Gorska K, et al. Reduction of neuropathic and inflammatory pain through inhibition of the tetrahydrobiopterin pathway. Neuron. 2015;86(6):1393-406.

41. Soda M, Hu D, Endo S, Takemura M, Li J, Wada R, et al. Design, synthesis and evaluation of caffeic acid phenethyl ester-based inhibitors targeting a selectivity pocket in the active site of human aldo-keto reductase 1B10. Eur J Med Chem. 2012;48:321-9.
42. Shi ZH, Li NG, Shi QP, Tang H, Tang YP, Li W, et al. Synthesis and structure-activity relationship analysis of caffeic acid amides as selective matrix metalloproteinase inhibitors. Bioorg Med Chem Lett. 2013;23(5):1206-11.
43. Dhagat U, Endo S, Hara A, El-Kabbani O. Inhibition of 3(17)alpha-hydroxysteroid dehydrogenase (AKR1C21) by aldose reductase inhibitors. Bioorg Med Chem. 2008;16(6):3245-54.
44. Wang L, Li X, Zhang S, Lu W, Liao S, Liu X, et al. Natural products as a gold mine for selective matrix metalloproteinases inhibitors. Bioorg Med Chem. 2012;20(13):4164-71.
45. Naeem S, Hylands P, Barlow D. Construction of an Indonesian herbal constituents database and its use in Random Forest modelling in a search for inhibitors of aldose reductase. Bioorg Med Chem. 2012;20(3):1251-8.
46. Jin GZ, Zhou QT, Chen LJ. New pharmacological effects of tetrahydroprotoberberines on dopamine receptor. Bull Nat Sci Found China. 2000;14(5):300-4.
47. Marengo A, Fumagalli M, Sanna C, Maxia A, Piazza S, Cagliero C, et al. The hydro-alcoholic extracts of Sardinian wild thistles (Onopordum spp.) inhibit TNFα-induced IL-8 secretion and NF-κB pathway in human gastric epithelial AGS cells. J Ethnopharmacol. 2018;210:469-76.
48. Bang BW, Park D, Kwon KS, Lee DH, Jang MJ, Park SK, et al. BST-104, a water extract of lonicera japonica, has a gastroprotective effect via antioxidant and anti-inflammatory activities. J Med Food. 2019;22(2):140-51.
49. da Cunha FM, Duma D, Assreuy J, Buzzi FC, Niero R, Campos MM, et al. Caffeic acid derivatives: in vitro and in vivo anti-inflammatory properties. Free Radic Res. 2004;38(11):1241-53.
50. Yang WS, Jeong D, Yi YS, Park JG, Seo H, Moh SH, et al. IRAK1/4-targeted anti-inflammatory action of caffeic acid. Mediators Inflamm. 2013;2013:518183.
51. Zhou L, Hu Y, Li C, Yan Y, Ao L, Yu B, et al. Levo-corydalmine alleviates vincristine-induced neuropathic pain in mice by inhibiting an NF-kappa B-dependent CXCL1/CXCR2 signaling pathway. Neuropharmacology. 2018;135:34-47.
52. Ma ZZ, Xu W, Jensen NH, Roth BL, Liu-Chen LY, Lee DY. Isoquinoline alkaloids isolated from Corydalis yanhusuo and their binding affinities at the dopamine D1 receptor. Molecules. 2008;13(9):2303-12.
53. Zhang S, Huang J, Xie X, He Y, Mo F, Luo Z. Quercetin from Polygonum capitatum Protects against Gastric Inflammation and Apoptosis Associated with Helicobacter pylori Infection by Affecting the Levels of p38MAPK, BCL-2 and BAX. Molecules. 2017;22(5):744.
54. Yeon MJ, Lee MH, Kim DH, Yang JY, Woo HJ, Kwon HJ, et al. Anti-inflammatory effects of Kaempferol on Helicobacter pylori-induced inflammation. Biosci Biotechnol Biochem. 2019;83(1):166-73.
55. Kim SH, Park JG, Sung GH, Yang S, Yang WS, Kim E, et al. Kaempferol, a dietary flavonoid, ameliorates acute inflammatory and nociceptive symptoms in gastritis, pancreatitis, and abdominal pain. Mol Nutr Food Res. 2015;59(7):1400-5.